Feasibility-driven Design of Reflectarrays: An Innovative Inverse Source Approach

M. Salucci, G. Oliveri, and A. Massa

Contents

Part I

Mathematical Formulation

1 Glossary

- Φ: Cost Function;
- A: Area of the reflectarray;
- q: type of polarization;
- α: complex coefficient;
- $J_p^{type}(.)$: some type (total, minimum-norm, non-radiating) of current;
- ϕ: phase;
- ξ: far-field integral error;
- M: number of elements along x;
- N: number of elements along y;
- Δx: element spacing along x [λ];
- Δy: element spacing along y [λ];
- H: truncation order;
- P: swarm size;
- I: max iteration number;
- K: number of NR-Basis (number of unknown).

2 Cost Function Definition

In this Section is defined the Cost function for the Simple Shaping objective in the scalar formulation. The aim of the objective is to have a total current distribution in which the

The cost function for the Simple Shaping objective in the scalar formulation is defined as:

$$\Phi\left(\underline{\alpha}\right)=\frac{\int\int_{A}\mathcal{H}\left[\angle\left\{J_{q}^{TOT}\left(x,y|\underline{\alpha}\right)\right\}-\phi_{q}^{MAX}\left(x,y\right)\right]+\mathcal{H}\left[\phi_{q}^{MIN}\left(x,y\right)-\angle\left\{J_{q}^{TOT}\left(x,y|\underline{\alpha}\right)\right\}\right]\,\mathrm{dxdy}}{\int\int_{A}\mathcal{H}\left[\angle\left\{J_{q}^{MN}\left(x,y\right)\right\}-\phi_{q}^{MAX}\left(x,y\right)\right]+\mathcal{H}\left[\phi_{q}^{MIN}\left(x,y\right)-\angle\left\{J_{q}^{MN}\left(x,y\right)\right\}\right]\,\mathrm{dxdy}} \quad (1)$$

where

- $\mathcal{H}\left[a-b\right]=\begin{cases}(a-b) & \text{if } a>b\\ 0 & \text{otherwise}\end{cases}$
- A: Area of the reflectarray;
- p: type of polarization;
- $\underline{\alpha}$: complex vector of coefficient (of dimension K);
- $J_{q}^{TOT}\left(x,y|\underline{\alpha}\right)$: total current of a given polarization (p);
- $\phi_{q}^{MIN}\left(x,y\right)$: user defined mask for the minimum phase of total current $J_{q}^{TOT}\left(x,y|\underline{\alpha}\right)$;
- $\phi_{q}^{MAX}\left(x,y\right)$: user defined mask for the maximum phase of total current $J_{q}^{TOT}\left(x,y|\underline{\alpha}\right)$.

3 Metrics for estimating the errors

3.1 Far-field mismatch

The following metric will be computed in order to check the mismatch between a given far-field $\underline{E}_{FF}\left(u,v\right)$ and a reference far-field $\underline{E}_{FF}^{ref}\left(u,v\right)$:

Far-field integral error:

$$\xi=\frac{\int_{u}\int_{v}\left|\underline{E}_{FF}\left(u,v\right)-\underline{E}_{FF}^{ref}\left(u,v\right)\right|\,dudv}{\int_{u}\int_{v}\underline{E}_{FF}^{ref}\left(u,v\right)\,dudv} \quad (2)$$

3.2 Phase Mask mismatch

The following metric will be computed in order to check the mismatch between the phase of a current and the Phase Mask:

Phase Mask mismatch:

$$\hat{\delta}^{MN/TOT}\left(x,y\right)=\begin{cases}\left|\mathcal{H}\left[\angle\left\{J_{q}^{MN/TOT}\left(x,y\right)\right\}-\phi_{q}^{MAX}\left(x,y\right)\right]\right| & if\,\angle\left\{J_{q}^{MN/TOT}\left(x,y\right)\right\}>0\\ \left|\mathcal{H}\left[\angle\left\{J_{q}^{MN/TOT}\left(x,y\right)\right\}-\phi_{q}^{MIN}\left(x,y\right)\right]\right| & if\,\angle\left\{J_{q}^{MN/TOT}\left(x,y\right)\right\}<0\end{cases} \quad (3)$$

Part II

Numerical Analysis

4 Phase Range [-90:90] - Test Case 1 - 55x55 - Linear Polarization

This section is aimed at showing the result of setting the wanted phase range to $[-90, 90]$ using a PSO with different parameters.

4.1 Parameters

- Reflectarray Geometry:
  - number of elements along x: $M = 55$;
  - number of elements along y: $N = 55$;
  - element spacing along x: $\Delta x = 0.373333$ [λ];
  - element spacing along y: $\Delta y = 0.373333$ [λ];
  - non radiating dimension: 2337;
  - truncation order: $H = 688$;
- PSO Parameters
  - max iteration number: $I = \{2 \times 10^4, 10^5\}$;
  - number of NR-Basis: $K = \{100, 200, 400, 800, 2000\}$;
  - swarm size:
    - for $K = \{100, 200\}$: $P = \{10, 20, 40\}$;
    - for $K = \{400\}$: $P = \{10, 20, 40, 100, 200\}$;
    - for $K = \{800, 2000\}$: $P = \{\frac{K}{8}, \frac{K}{4}, \frac{K}{2}\}$;
  - inertial weight: 0.4;
  - inertial: 2 -> consider constant inertial velocity;
  - alpha: 0.4,
  - beta: 0.4;
  - c1: 2.0;
  - c2: 2.0;
  - random seed: {1, 2}.
- Optimization Parameters
  - $\phi_q^{MAX}(x, y) = 90$ [deg];
  - $\phi_q^{MIN}(x, y) = -90$ [deg];
  - $\min\{\Re\{\underline{\alpha}\}\} = -1.0$;

- $\max\{\Re\{\underline{\alpha}\}\} = 1.0$;
- $\min\{\Im\{\underline{\alpha}\}\} = -1.0$;
- $\max\{\Im\{\underline{\alpha}\}\} = 1.0$.

Initialialization We use a population with:

- an agent with the $\underline{\alpha} = \underline{0}$,
- all the other agents with random initialized $\underline{\alpha}$.

4.2 K=100, P=10, I=20000

In the Fig. 1 is depicted the behaviour of the Cost Function varying the random seed. The best value of cost function is achieved by Seed=2 and is $\Phi = 7.472 \times 10^{-1}$.

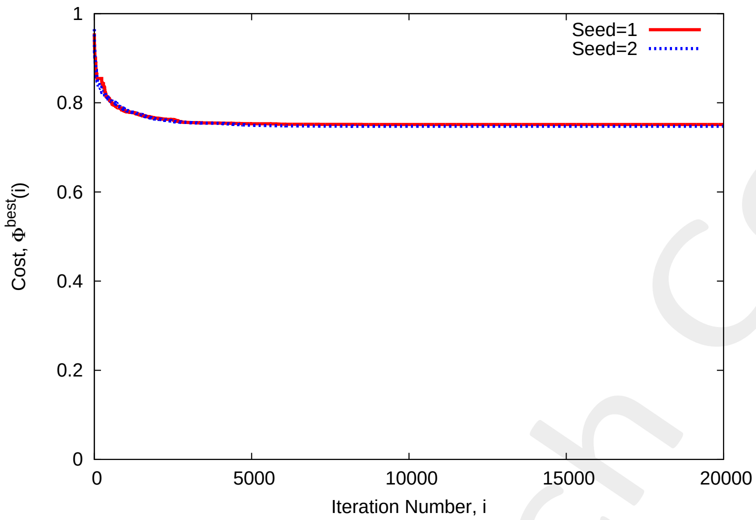

Figure 1: Cost Function behaviour at different random seed.

At this value of cost function the achieved performance on the Phase are showed in Fig. 2 and are numerically showed in table I.

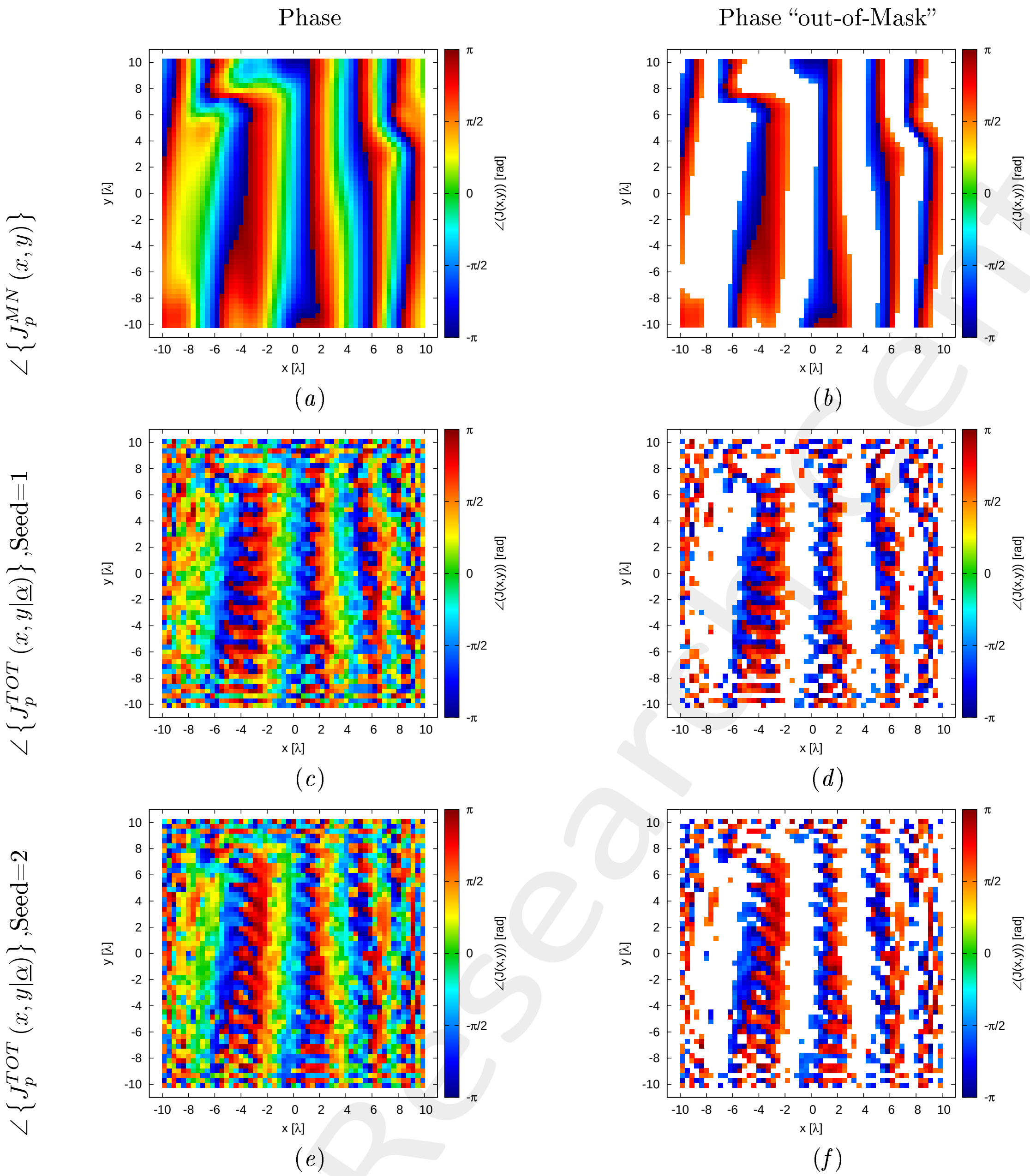

Figure 2: Phase $(a)(c)(e)$ and value of the phase out of the minimization range $(b)(d)(f)$ of the Minimum-Norm current $(\angle\left\{J_p^{MN}(x,y)\right\})(a)(b)$, of the total current for the random seed $=1(c)(d)$ and for the random seed $=2(e)(f)$.

Case	Φ	Number of value $> \phi_p^{MAX}(x,y)$	Number of value $< \phi_p^{MIN}(x,y)$	Phase Range		Time $[s]$
				Min $[deg]$	Max $[deg]$	
MN	1.0	899	663	-179.87	179.63	
Seed=1	7.513×10^{-1}	756	666	-179.63	179.34	6.26×10^{2}
Seed=2	7.472×10^{-1}	782	661	-179.77	179.67	6.26×10^{2}

Table I: Cost Function value and statistics about the result.

The verification of the radiated field is showed in Fig. 3 and numerically in table II.

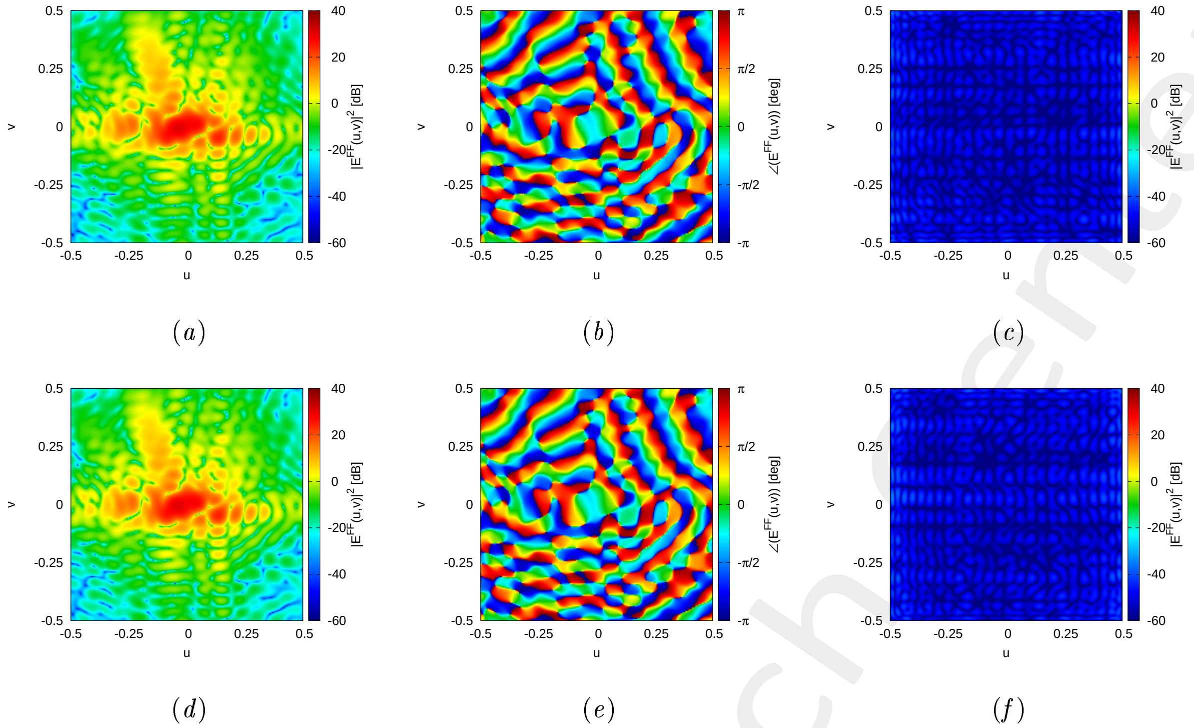

Figure 3: Magnitude $(a)(d)$, Phase $(b)(e)$ and Magnitude of the difference with respect to the original field $(c)(f)$ of the seed=1 $(a)(b)(c)$ and seed=2 $(d)(e)(f)$.

Seed	ξ
1	2.02×10^{-3}
2	2.18×10^{-3}

Table II: Integral error of the difference between the original field and the one radiated by the total current.

4.3 K=100, P=20, I=20000

In the Fig. 4 is depicted the behaviour of the Cost Function varying the random seed. The best value of cost function is achieved by Seed=2 and is $\Phi = 7.074 \times 10^{-1}$.

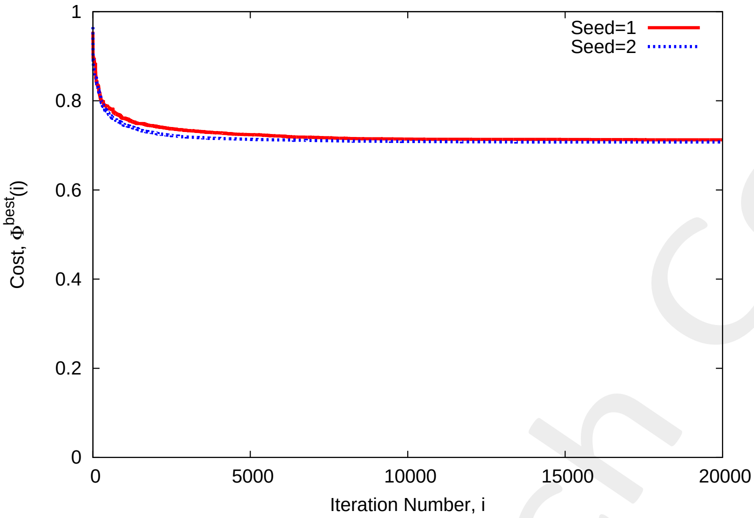

Figure 4: Cost Function behaviour at different random seed.

At this value of cost function the achieved performance on the Phase are showed in Fig. 5 and are numerically showed in table III.

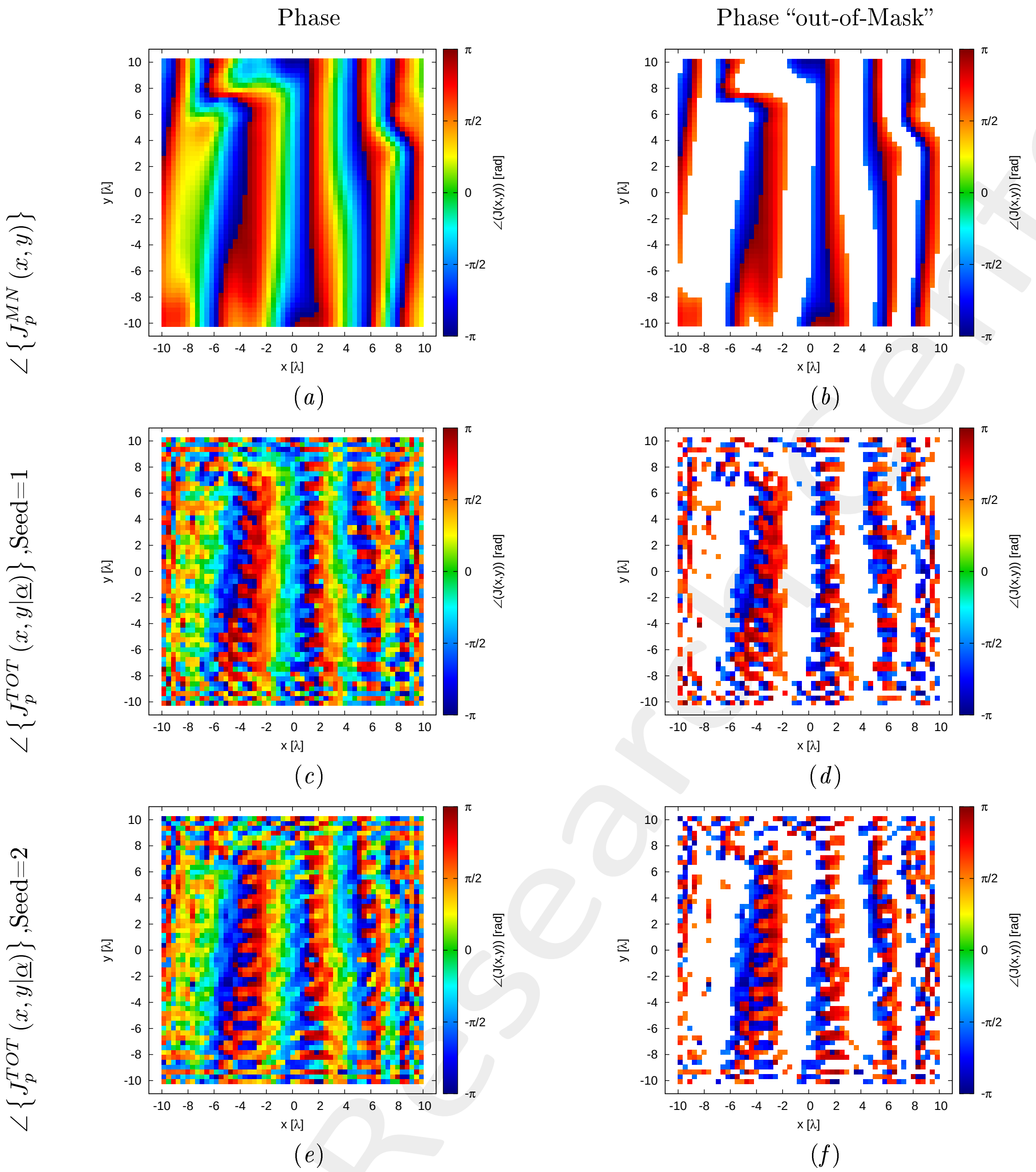

Figure 5: Phase $(a)(c)(e)$ and value of the phase out of the minimization range $(b)(d)(f)$ of the Minimum-Norm current $(\angle\{J_p^{MN}(x,y)\})(a)(b)$, of the total current for the random seed $= 1(c)(d)$ and for the random seed $= 2(e)(f)$.

Case	Φ	Number of value $> \phi_p^{MAX}(x,y)$	Number of value $< \phi_p^{MIN}(x,y)$	Phase Range		Time $[s]$
				Min $[deg]$	Max $[deg]$	
MN	1.0	899	663	-179.87	179.63	
Seed=1	7.123×10^{-1}	784	623	-179.33	179.20	1.36×10^{3}
Seed=2	7.074×10^{-1}	748	646	-179.84	179.91	1.30×10^{3}

Table III: Cost Function value and statistics about the result.

The verification of the radiated field is showed in Fig. 6 and numerically in table IV.

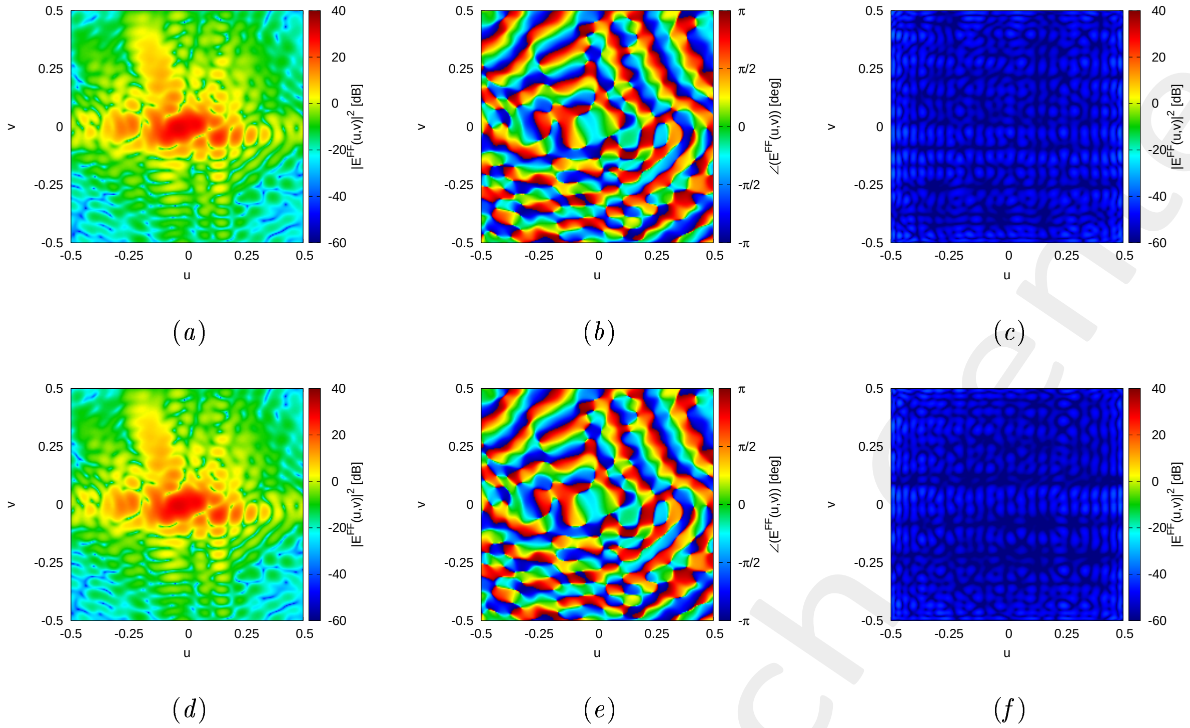

Figure 6: Magnitude $(a)(d)$, Phase $(b)(e)$ and Magnitude of the difference with respect to the original field $(c)(f)$ of the seed=1 $(a)(b)(c)$ and seed=2 $(d)(e)(f)$.

Seed	ξ
1	2.22×10^{-3}
2	2.01×10^{-3}

Table IV: Integral error of the difference between the original field and the one radiated by the total current.

4.4 K=100, P=40, I=20000

In the Fig. 7 is depicted the behaviour of the Cost Function varying the random seed. The best value of cost function is achieved by Seed=2 and is $\Phi = 7.005 \times 10^{-1}$.

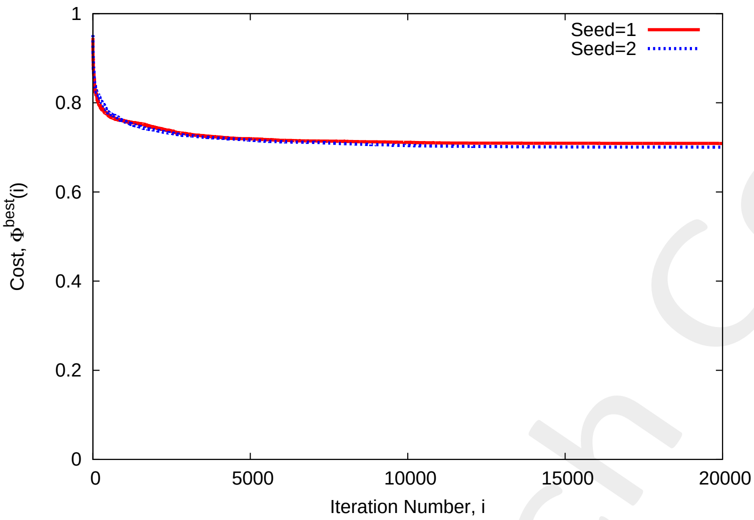

Figure 7: Cost Function behaviour at different random seed.

At this value of cost function the achieved performance on the Phase are showed in Fig. 8 and are numerically showed in table V.

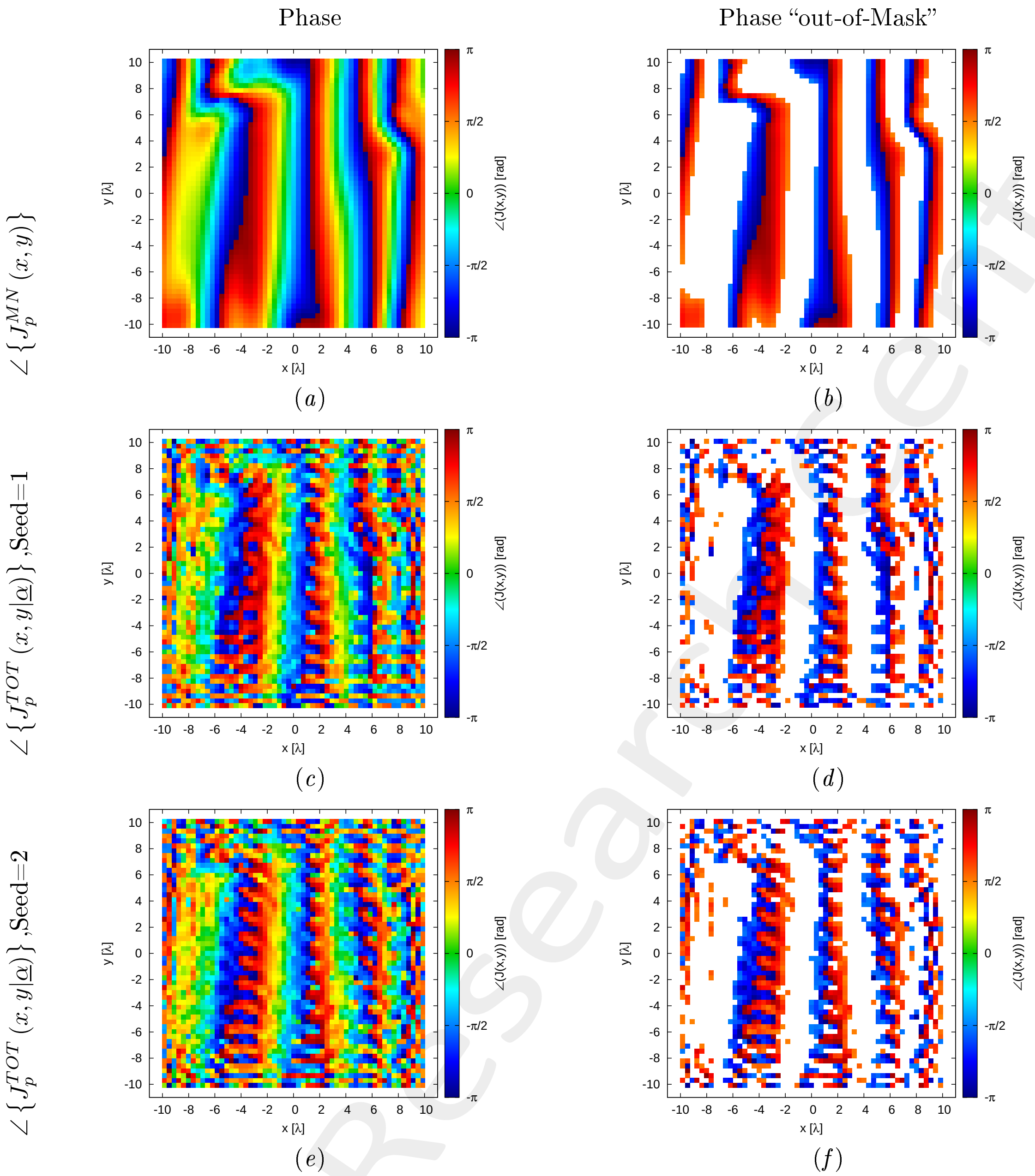

Figure 8: Phase $(a)(c)(e)$ and value of the phase out of the minimization range $(b)(d)(f)$ of the Minimum-Norm current $(\angle\left\{J_p^{MN}(x,y)\right\})(a)(b)$, of the total current for the random seed $=1(c)(d)$ and for the random seed $=2(e)(f)$.

Case	Φ	Number of value $> \phi_p^{MAX}(x,y)$	Number of value $< \phi_p^{MIN}(x,y)$	Phase Range		Time $[s]$
				Min $[deg]$	Max $[deg]$	
MN	1.0	899	663	-179.87	179.63	
Seed=1	7.088×10^{-1}	731	679	-179.41	179.72	2.64×10^{3}
Seed=2	7.005×10^{-1}	748	668	-179.81	179.96	2.69×10^{3}

Table V: Cost Function value and statistics about the result.

The verification of the radiated field is showed in Fig. 9 and numerically in table VI.

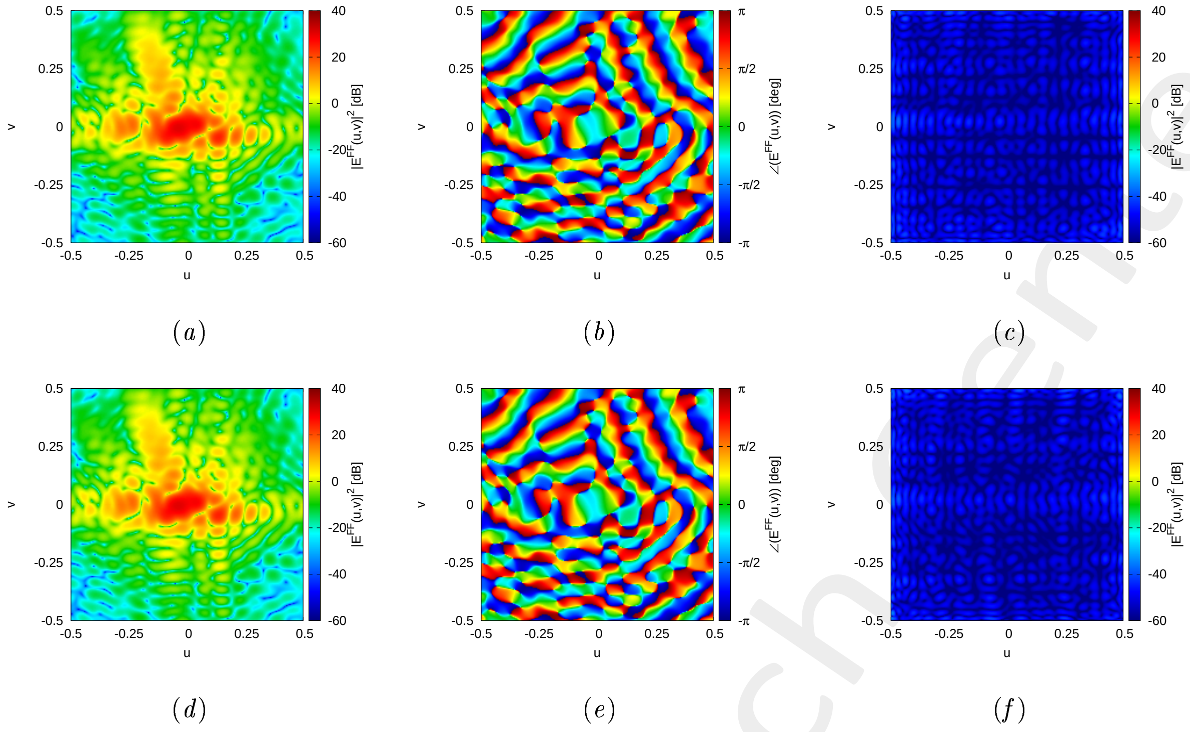

Figure 9: Magnitude $(a)(d)$, Phase $(b)(e)$ and Magnitude of the difference with respect to the original field $(c)(f)$ of the seed=1 $(a)(b)(c)$ and seed=2 $(d)(e)(f)$.

Seed	ξ
1	1.95×10^{-3}
2	1.88×10^{-3}

Table VI: Integral error of the difference between the original field and the one radiated by the total current.

4.5 K=200, P=10, I=20000

In the Fig. 10 is depicted the behaviour of the Cost Function varying the random seed. The best value of cost function is achieved by Seed=1 and is $\Phi = 7.070 \times 10^{-1}$.

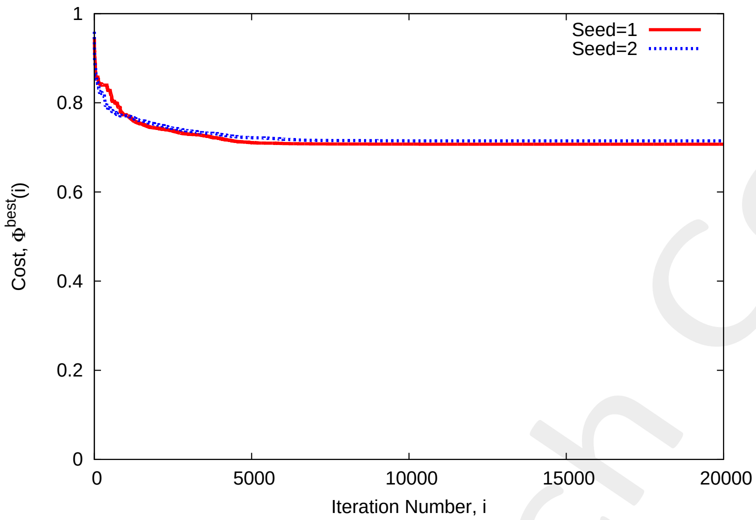

Figure 10: Cost Function behaviour at different random seed.

At this value of cost function the achieved performance on the Phase are showed in Fig. 11 and are numerically showed in table VII.

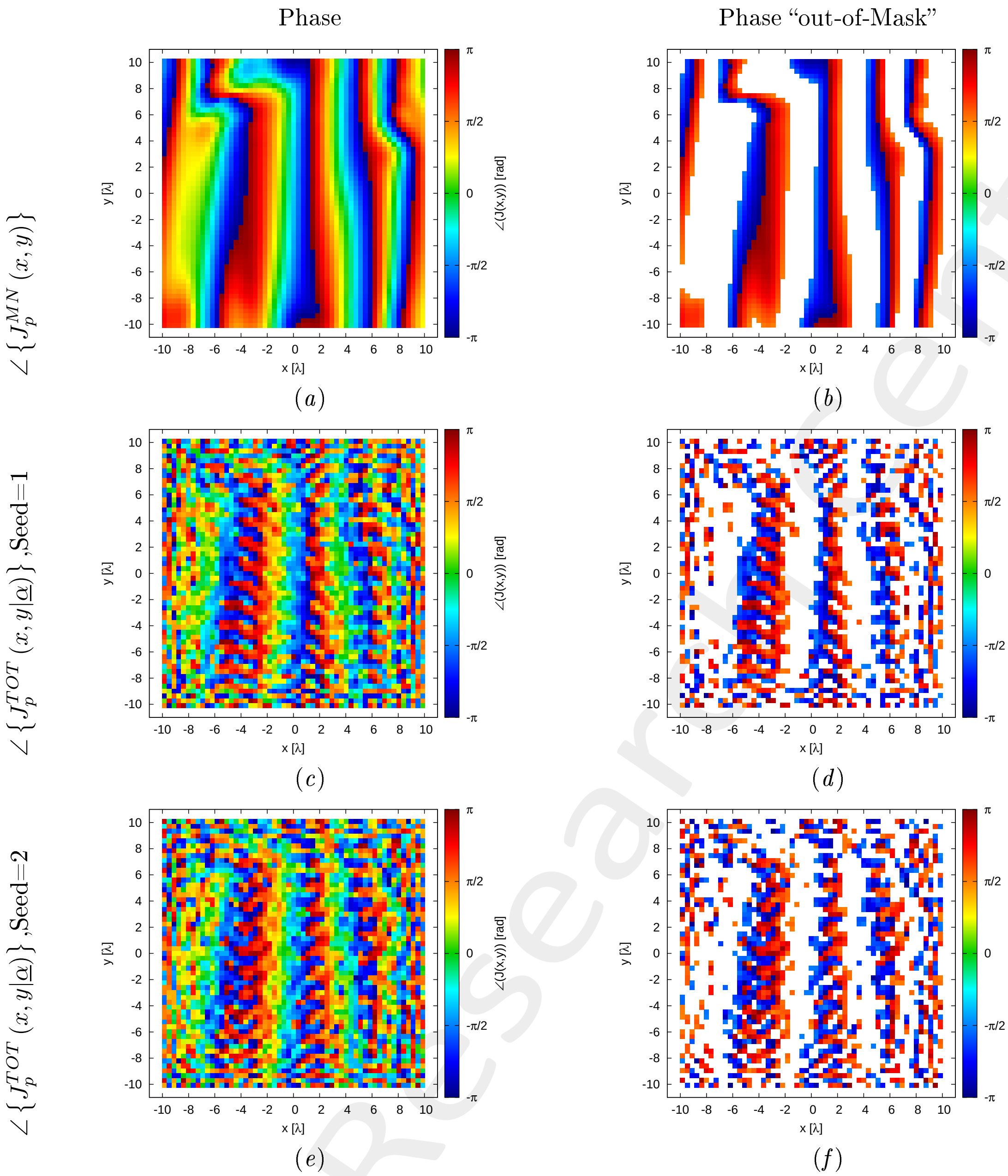

Figure 11: Phase $(a)(c)(e)$ and value of the phase out of the minimization range $(b)(d)(f)$ of the Minimum-Norm current $(\angle\left\{J_p^{MN}(x,y)\right\})(a)(b)$, of the total current for the random seed $=1(c)(d)$ and for the random seed $=2(e)(f)$.

Case	Φ	Number of value $> \phi_p^{MAX}(x,y)$	Number of value$< \phi_p^{MIN}(x,y)$	Phase Range		Time $[s]$
				Min $[deg]$	Max $[deg]$	
MN	1.0	899	663	-179.87	179.63	
Seed=1	7.070×10^{-1}	724	683	-179.51	179.27	1.23×10^{3}
Seed=2	7.145×10^{-1}	749	689	-179.28	179.27	1.23×10^{3}

Table VII: Cost Function value and statistics about the result.

The verification of the radiated field is showed in Fig. 12 and numerically in table VIII.

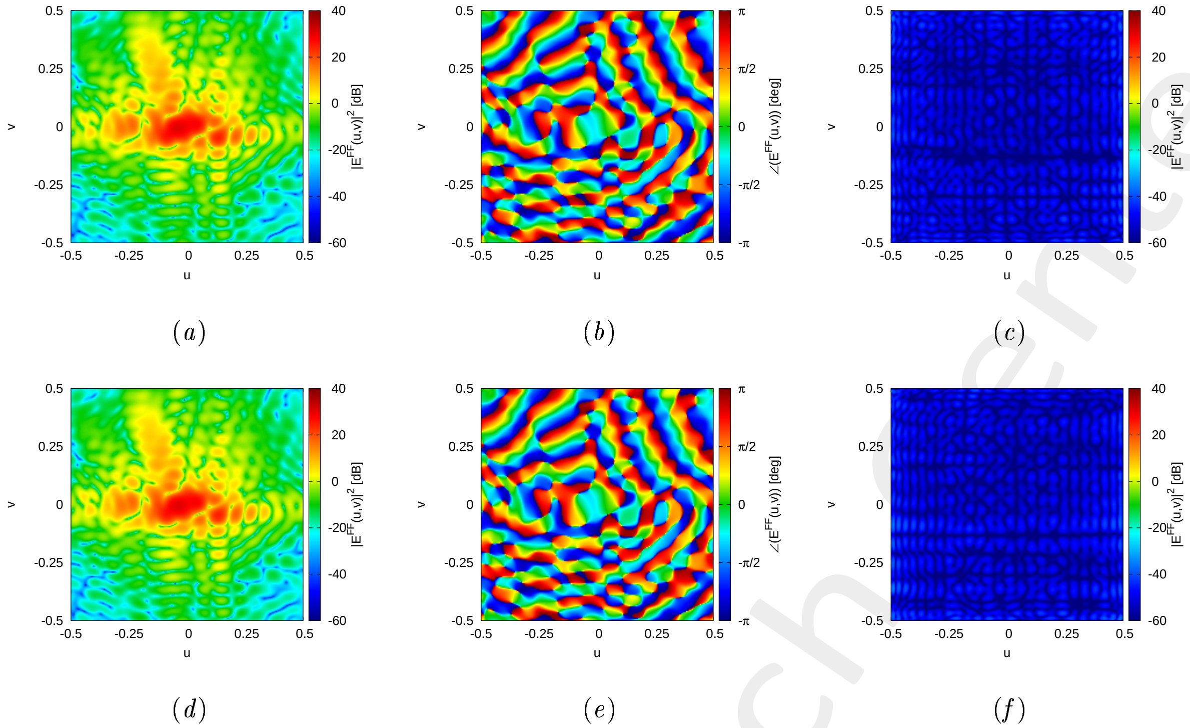

Figure 12: Magnitude $(a)(d)$, Phase $(b)(e)$ and Magnitude of the difference with respect to the original field $(c)(f)$ of the seed=1 $(a)(b)(c)$ and seed=2 $(d)(e)(f)$.

Seed	ξ
1	2.02×10^{-3}
2	2.07×10^{-3}

Table VIII: Integral error of the difference between the original field and the one radiated by the total current.

4.6 K=200, P=20, I=20000

In the Fig. 13 is depicted the behaviour of the Cost Function varying the random seed. The best value of cost function is achieved by Seed=2 and is $\Phi = 6.623 \times 10^{-1}$.

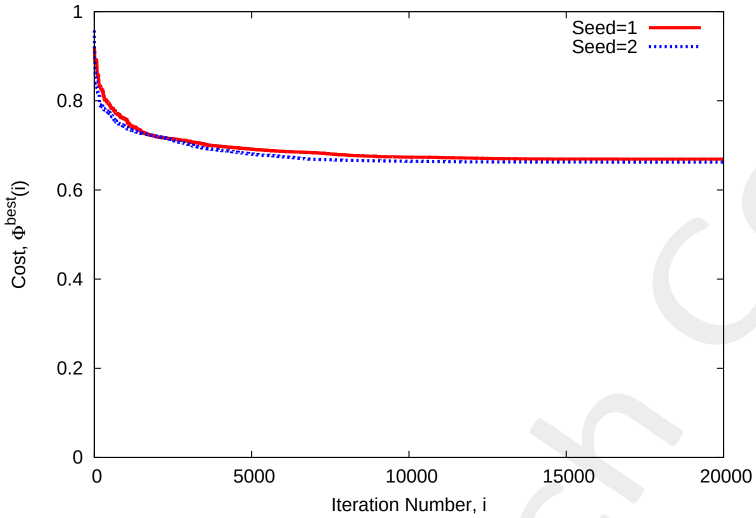

Figure 13: Cost Function behaviour at different random seed.

At this value of cost function the achieved performance on the Phase are showed in Fig. 14 and are numerically showed in table IX.

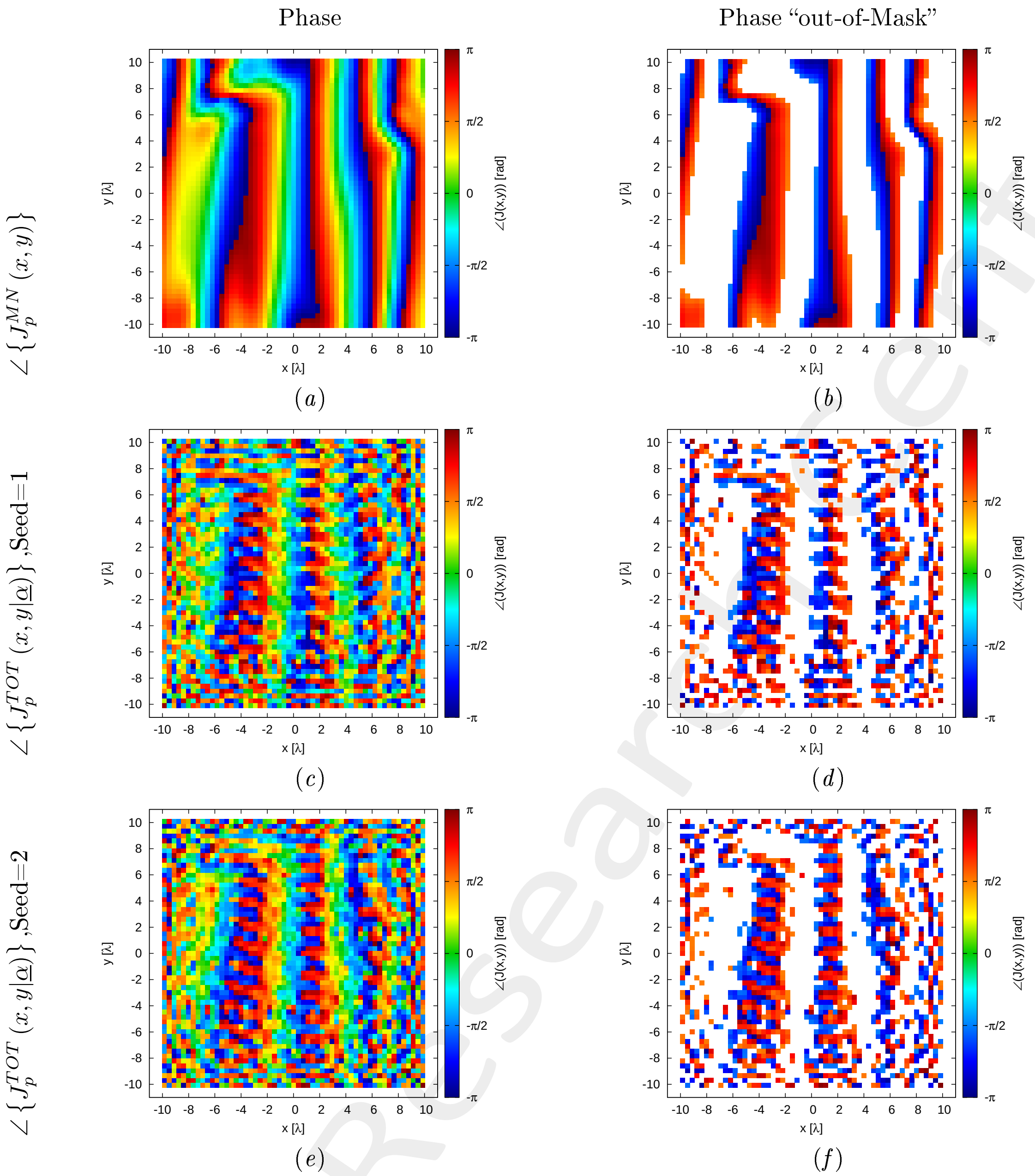

Figure 14: Phase $(a)(c)(e)$ and value of the phase out of the minimization range $(b)(d)(f)$ of the Minimum-Norm current $(\angle\left\{J_p^{MN}(x,y)\right\})(a)(b)$, of the total current for the random seed $= 1(c)(d)$ and for the random seed $= 2(e)(f)$.

Case	Φ	Number of value $> \phi_p^{MAX}(x,y)$	Number of value $< \phi_p^{MIN}(x,y)$	Phase Range		Time $[s]$
				Min $[deg]$	Max $[deg]$	
MN	1.0	899	663	-179.87	179.63	
Seed=1	6.691×10^{-1}	757	639	-179.43	179.66	2.45×10^{3}
Seed=2	6.623×10^{-1}	745	623	-179.72	179.77	2.45×10^{3}

Table IX: Cost Function value and statistics about the result.

The verification of the radiated field is showed in Fig. 15 and numerically in table X.

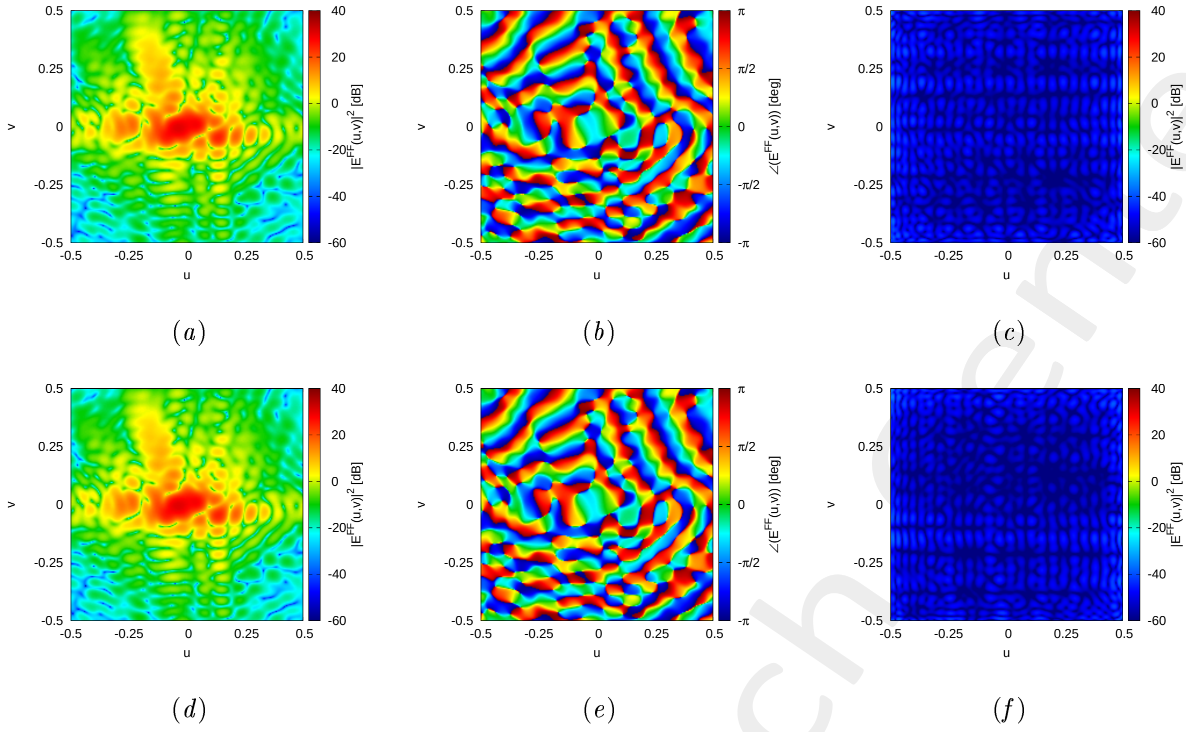

Figure 15: Magnitude $(a)(d)$, Phase $(b)(e)$ and Magnitude of the difference with respect to the original field $(c)(f)$ of the seed=1 $(a)(b)(c)$ and seed=2 $(d)(e)(f)$.

Seed	ξ
1	2.10×10^{-3}
2	1.97×10^{-3}

Table X: Integral error of the difference between the original field and the one radiated by the total current.

4.7 K=200, P=40, I=20000

In the Fig. 16 is depicted the behaviour of the Cost Function varying the random seed. The best value of cost function is achieved by Seed=1 and is $\Phi = 6.204 \times 10^{-1}$.

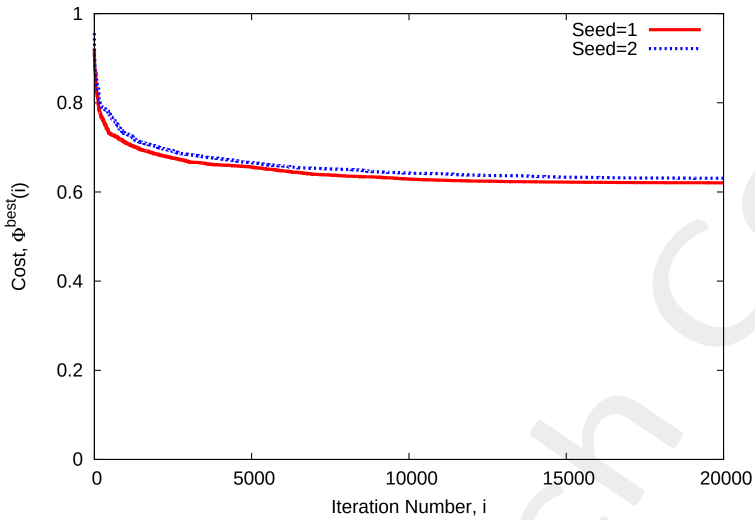

Figure 16: Cost Function behaviour at different random seed.

At this value of cost function the achieved performance on the Phase are showed in Fig. 17 and are numerically showed in table XI.

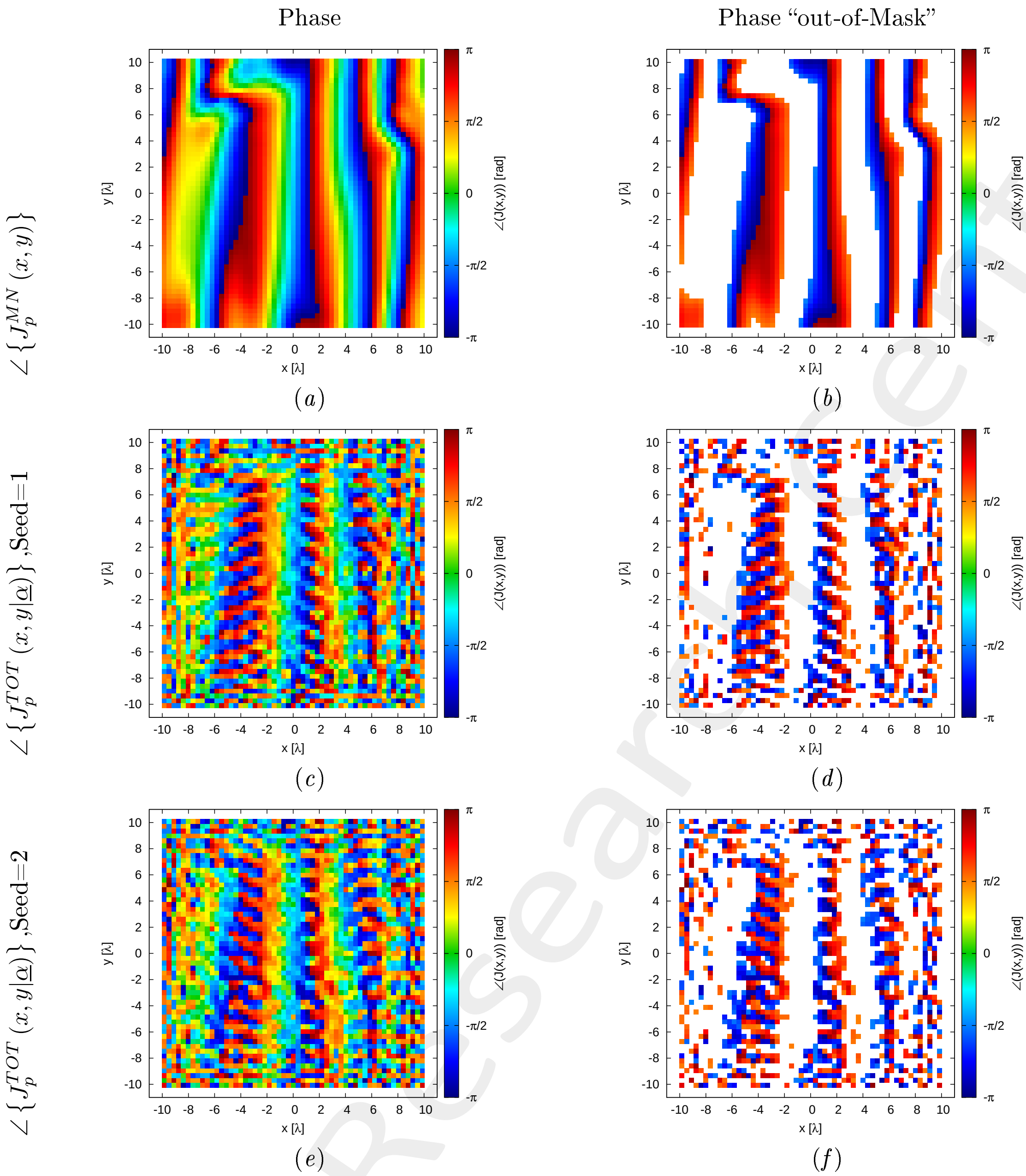

Figure 17: Phase $(a)(c)(e)$ and value of the phase out of the minimization range $(b)(d)(f)$ of the Minimum-Norm current $(\angle\left\{J_p^{MN}(x,y)\right\})(a)(b)$, of the total current for the random seed $=1(c)(d)$ and for the random seed $=2(e)(f)$.

Case	Φ	Number of value $> \phi_p^{MAX}(x,y)$	Number of value $< \phi_p^{MIN}(x,y)$	Phase Range		Time $[s]$
				Min $[deg]$	Max $[deg]$	
MN	1.0	899	663	-179.87	179.63	
Seed=1	6.204×10^{-1}	719	594	-179.96	179.54	4.63×10^{3}
Seed=2	6.307×10^{-1}	683	648	-179.56	179.63	4.61×10^{3}

Table XI: Cost Function value and statistics about the result.

The verification of the radiated field is showed in Fig. 18 and numerically in table XII.

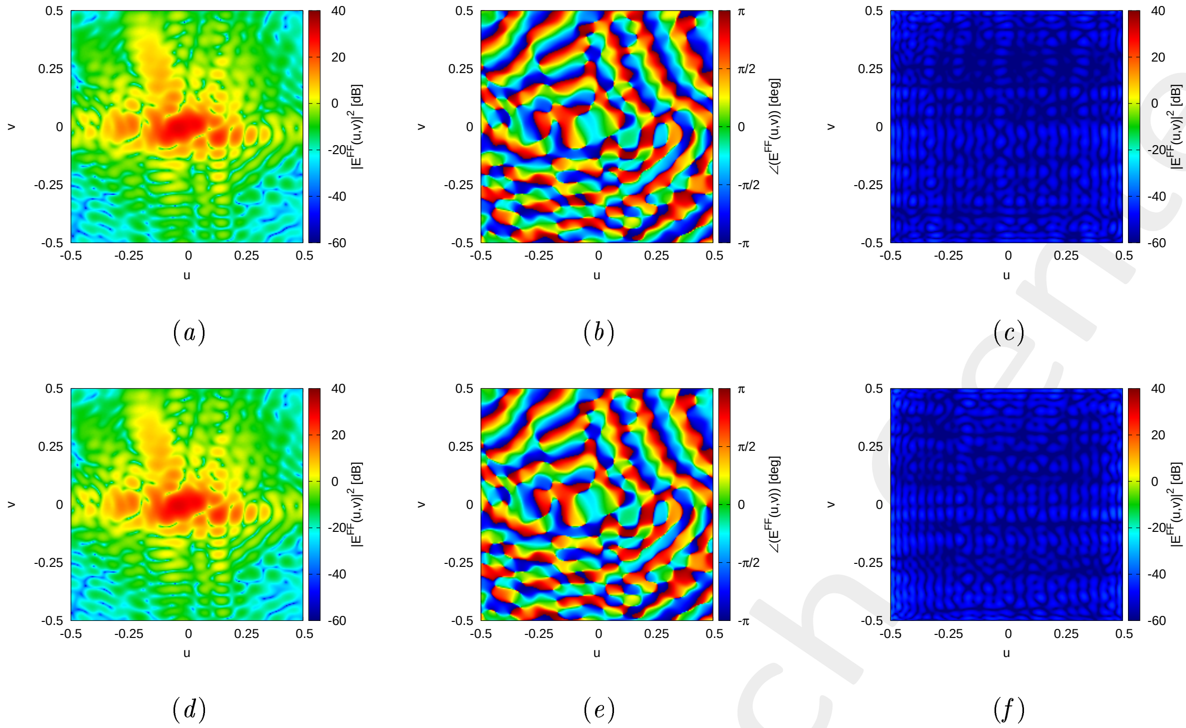

Figure 18: Magnitude $(a)(d)$, Phase $(b)(e)$ and Magnitude of the difference with respect to the original field $(c)(f)$ of the seed=1 $(a)(b)(c)$ and seed=2 $(d)(e)(f)$.

Seed	ξ
1	1.83×10^{-3}
2	1.97×10^{-3}

Table XII: Integral error of the difference between the original field and the one radiated by the total current.

4.8 K=400, P=10, I=20000

In the Fig. 19 is depicted the behaviour of the Cost Function varying the random seed. The best value of cost function is achieved by Seed=2 and is $\Phi = 6.873 \times 10^{-1}$.

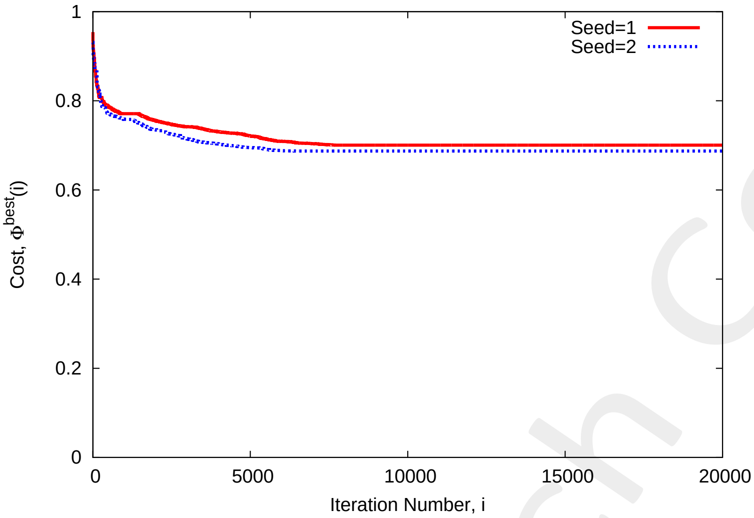

Figure 19: Cost Function behaviour at different random seed.

At this value of cost function the achieved performance on the Phase are showed in Fig. 20 and are numerically showed in table XIII.

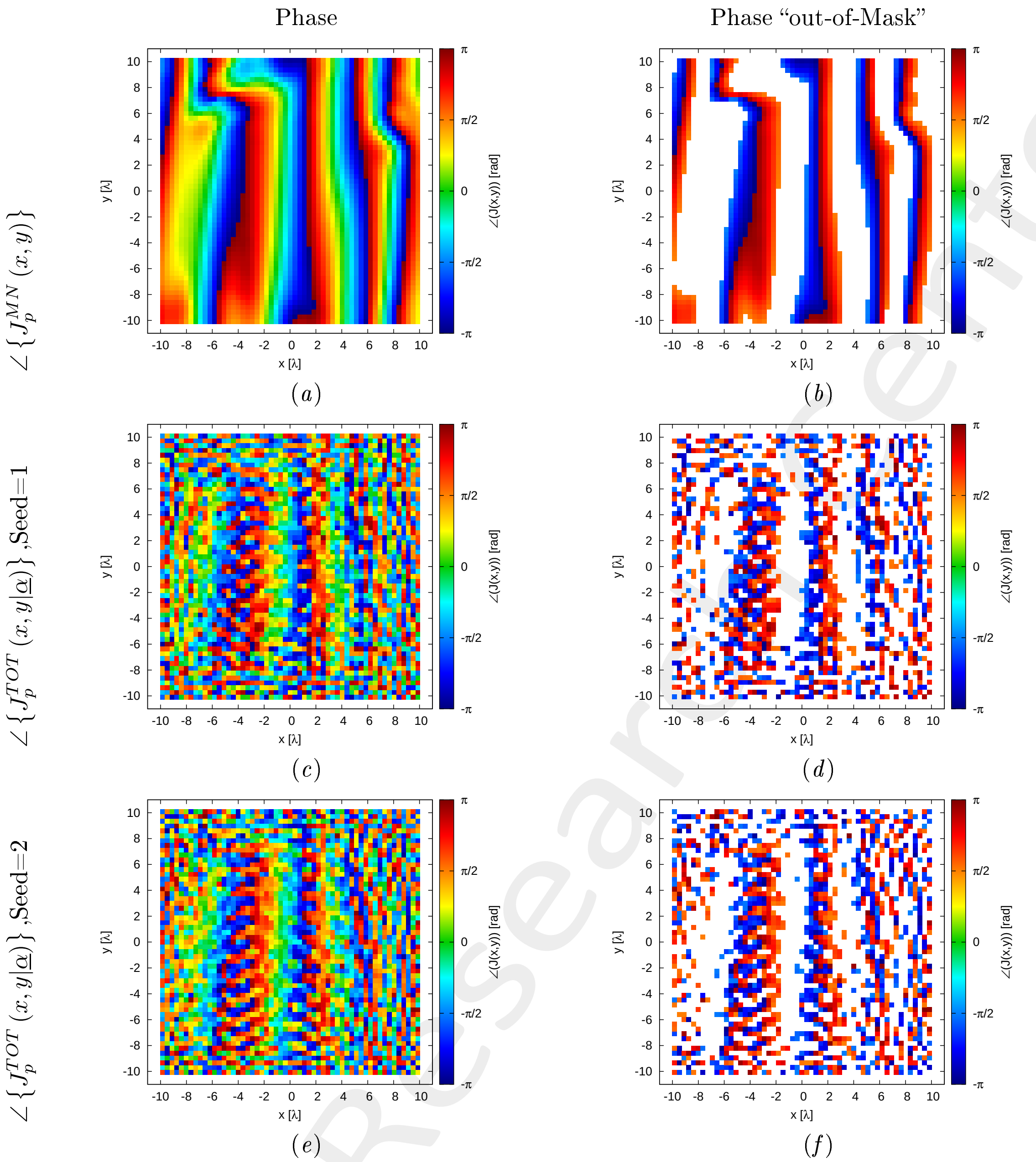

Figure 20: Phase $(a)(c)(e)$ and value of the phase out of the minimization range $(b)(d)(f)$ of the Minimum-Norm current $(\angle\{J_p^{MN}(x,y)\})(a)(b)$, of the total current for the random seed $= 1(c)(d)$ and for the random seed $= 2(e)(f)$.

Case	Φ	Number of value $> \phi_p^{MAX}(x,y)$	Number of value $< \phi_p^{MIN}(x,y)$	Phase Range		Time $[s]$
				Min $[deg]$	Max $[deg]$	
MN	1.0	899	663	-179.87	179.63	
Seed=1	7.004×10^{-1}	742	670	-179.74	180.00	2.36×10^{3}
Seed=2	6.873×10^{-1}	736	673	-179.28	178.38	2.33×10^{3}

Table XIII: Cost Function value and statistics about the result.

The verification of the radiated field is showed in Fig. 21 and numerically in table XIV.

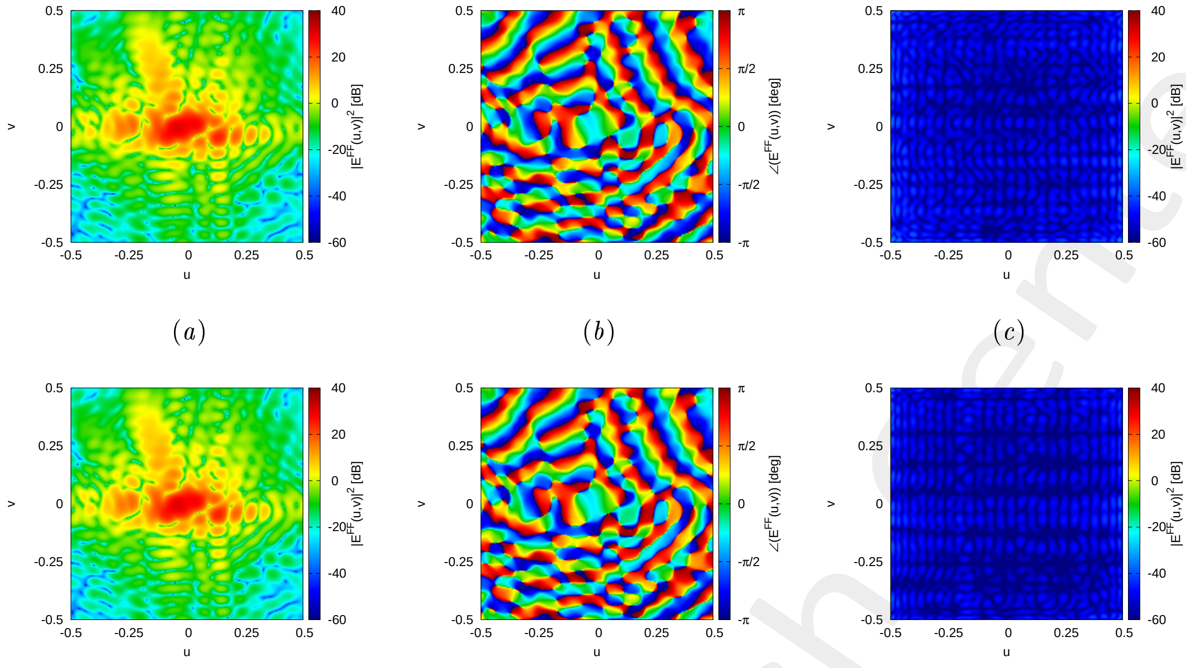

(a) (b) (c) (d) (e) (f)

Figure 21: Magnitude $(a)(d)$, Phase $(b)(e)$ and Magnitude of the difference with respect to the original field $(c)(f)$ of the seed=1 $(a)(b)(c)$ and seed=2 $(d)(e)(f)$.

Seed	ξ
1	2.22×10^{-3}
2	1.80×10^{-3}

Table XIV: Integral error of the difference between the original field and the one radiated by the total current.

4.9 K=400, P=20, I=20000

In the Fig. 22 is depicted the behaviour of the Cost Function varying the random seed. The best value of cost function is achieved by Seed=2 and is $\Phi = 6.255 \times 10^{-1}$.

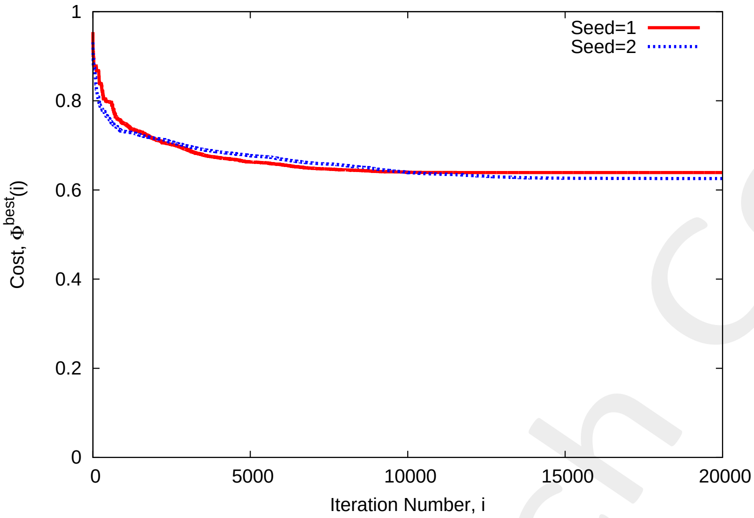

Figure 22: Cost Function behaviour at different random seed.

At this value of cost function the achieved performance on the Phase are showed in Fig. 23 and are numerically showed in table XV.

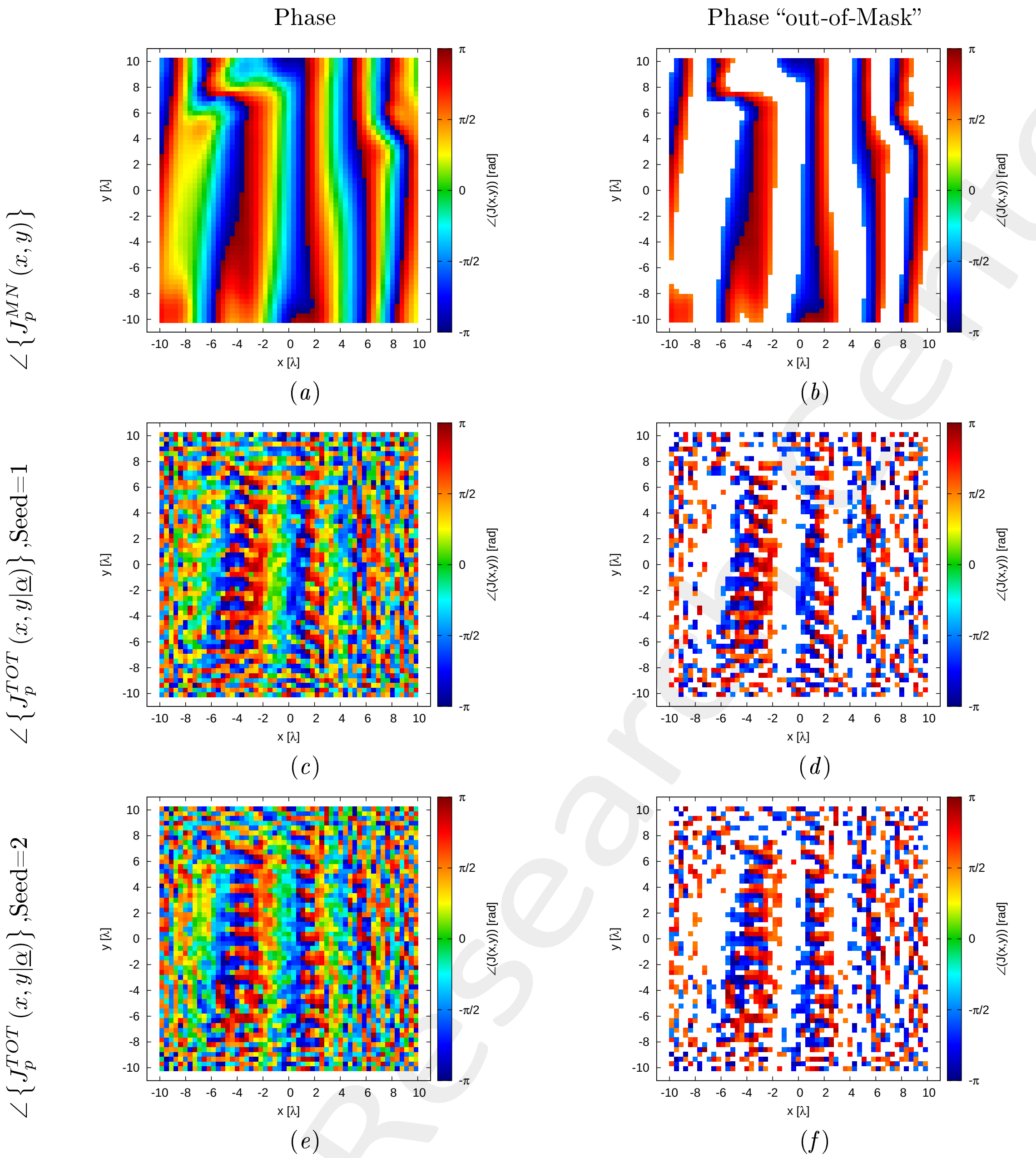

Figure 23: Phase $(a)(c)(e)$ and value of the phase out of the minimization range $(b)(d)(f)$ of the Minimum-Norm current $(\angle\left\{J_p^{MN}(x,y)\right\})(a)(b)$, of the total current for the random seed $= 1(c)(d)$ and for the random seed $= 2(e)(f)$.

Case	Φ	Number of value $> \phi_p^{MAX}(x,y)$	Number of value $< \phi_p^{MIN}(x,y)$	Phase Range		Time $[s]$
				Min $[deg]$	Max $[deg]$	
MN	1.0	899	663	-179.87	179.63	
Seed=1	6.391×10^{-1}	703	657	-178.88	179.50	4.66×10^3
Seed=2	6.255×10^{-1}	714	641	-178.98	178.82	4.66×10^3

Table XV: Cost Function value and statistics about the result.

The verification of the radiated field is showed in Fig. 24 and numerically in table XVI.

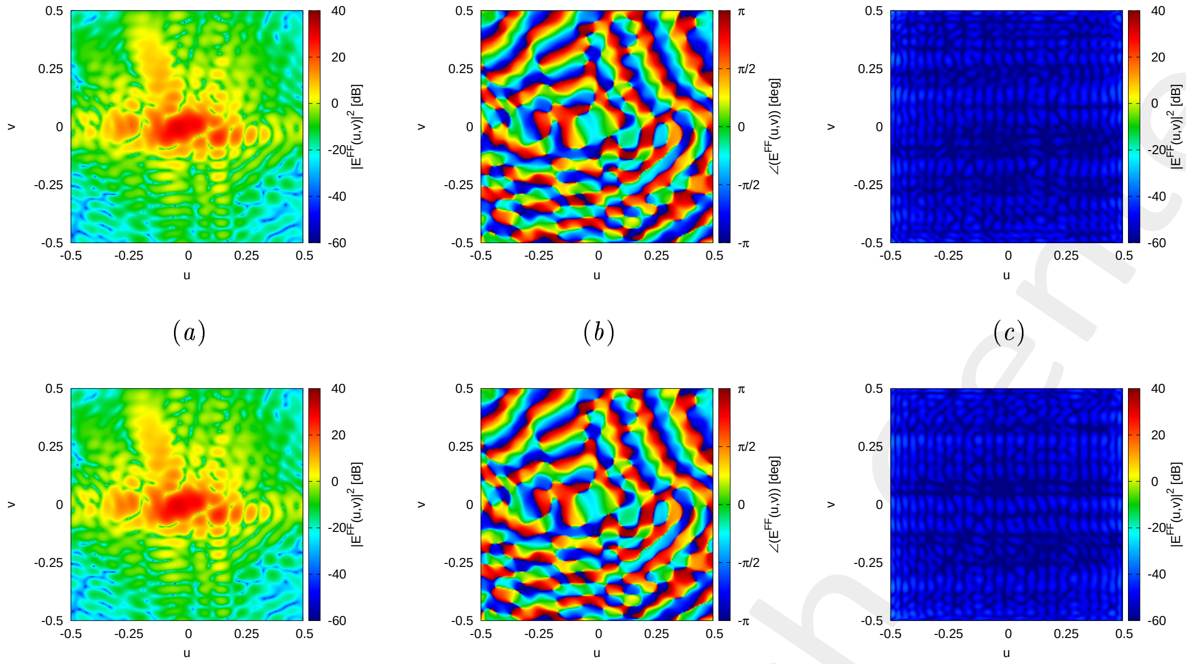

(a) (b) (c)

(d) (e) (f)

Figure 24: Magnitude $(a)(d)$, Phase $(b)(e)$ and Magnitude of the difference with respect to the original field $(c)(f)$ of the seed=1 $(a)(b)(c)$ and seed=2 $(d)(e)(f)$.

Seed	ξ
1	1.98×10^{-3}
2	2.14×10^{-3}

Table XVI: Integral error of the difference between the original field and the one radiated by the total current.

4.10 K=400, P=40, I=20000

In the Fig. 25 is depicted the behaviour of the Cost Function varying the random seed. The best value of cost function is achieved by Seed=2 and is $\Phi = 5.960 \times 10^{-1}$.

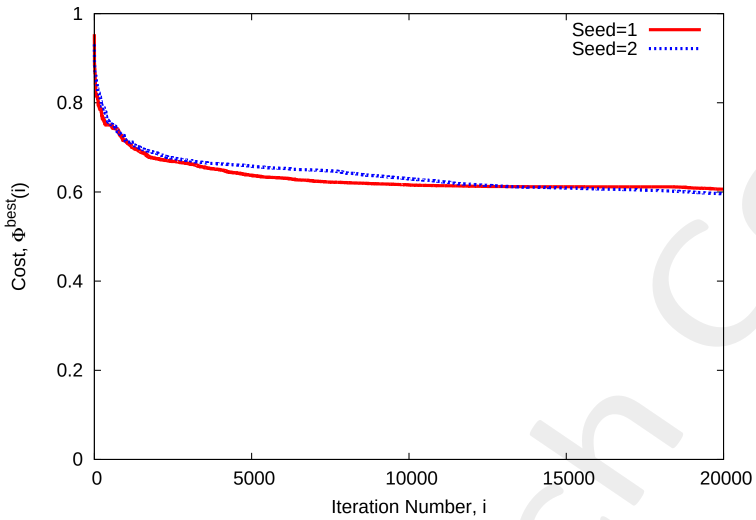

Figure 25: Cost Function behaviour at different random seed.

At this value of cost function the achieved performance on the Phase are showed in Fig. 26 and are numerically showed in table XVII.

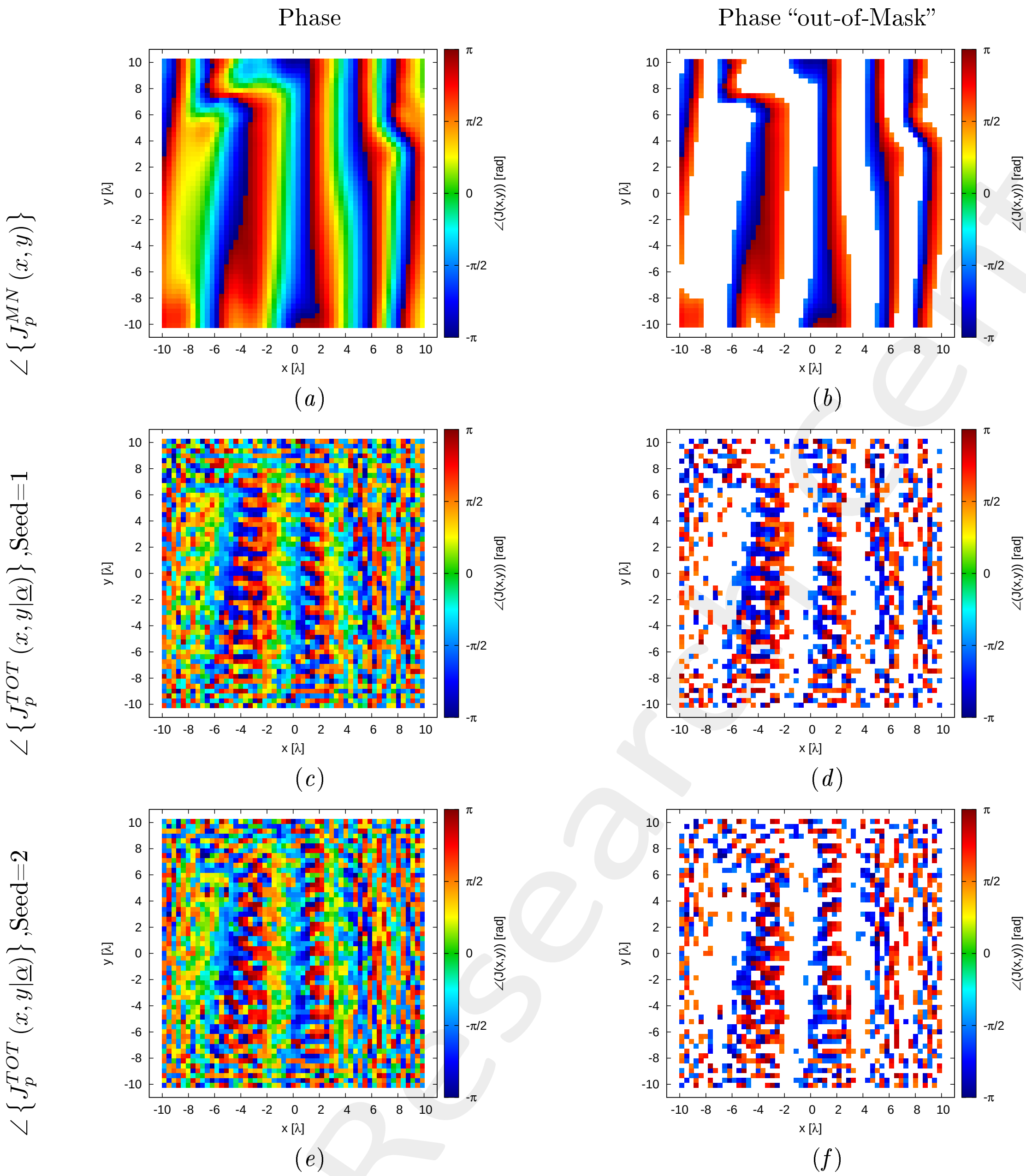

Figure 26: Phase $(a)(c)(e)$ and value of the phase out of the minimization range $(b)(d)(f)$ of the Minimum-Norm current $(\angle \left\{ J_p^{MN}(x,y) \right\})(a)(b)$, of the total current for the random seed $= 1(c)(d)$ and for the random seed $= 2(e)(f)$.

Case	Φ	Number of value $> \phi_p^{MAX}(x,y)$	Number of value$< \phi_p^{MIN}(x,y)$	Phase Range		Time $[s]$
				Min $[deg]$	Max $[deg]$	
MN	1.0	899	663	-179.87	179.63	
Seed=1	6.062×10^{-1}	686	634	-179.95	178.81	9.36×10^{3}
Seed=2	5.960×10^{-1}	681	608	-179.94	179.54	9.43×10^{3}

Table XVII: Cost Function value and statistics about the result.

The verification of the radiated field is showed in Fig. 27 and numerically in table XVIII.

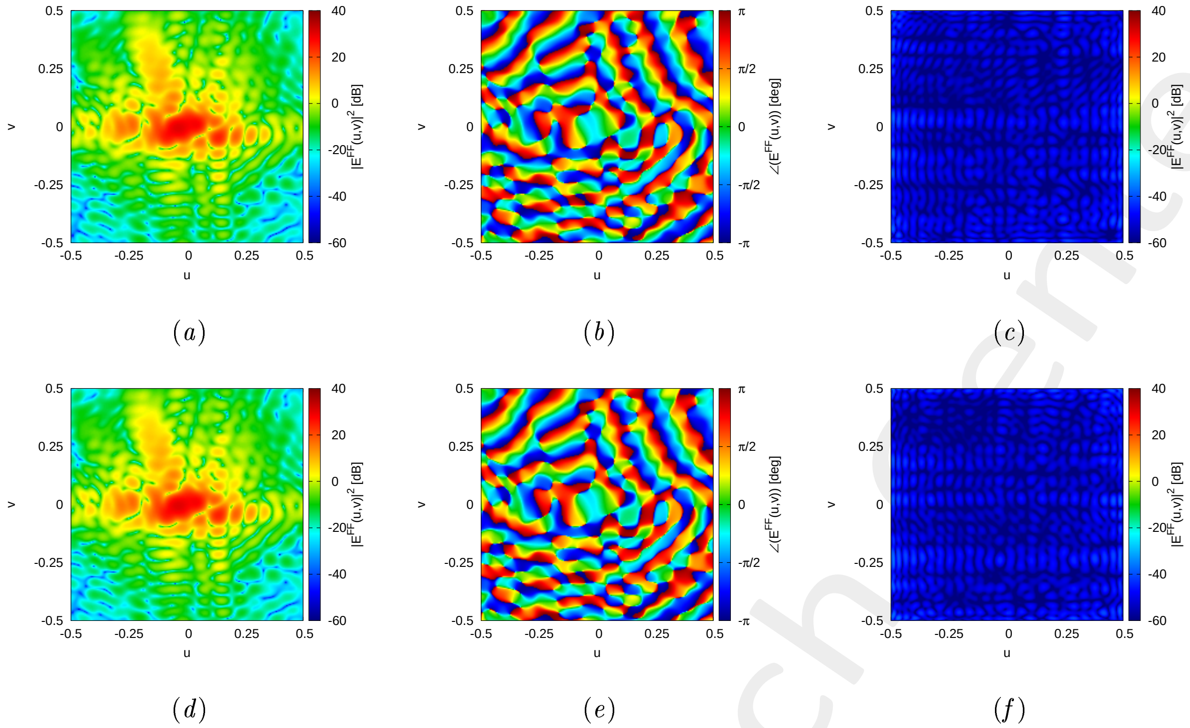

Figure 27: Magnitude $(a)(d)$, Phase $(b)(e)$ and Magnitude of the difference with respect to the original field $(c)(f)$ of the seed=1 $(a)(b)(c)$ and seed=2 $(d)(e)(f)$.

Seed	ξ
1	1.92×10^{-3}
2	1.96×10^{-3}

Table XVIII: Integral error of the difference between the original field and the one radiated by the total current.

4.11 Comparison

In the Fig. 28 is depicted a summary of the behaviour of the cost function at diffenent population and number of coefficient and seed.

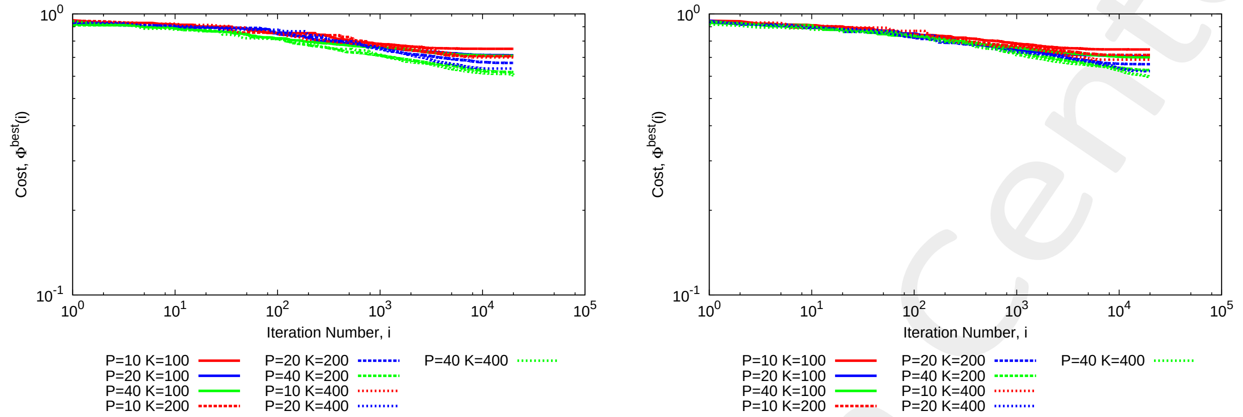

(a) (b)

Figure 28: Cost Function behaviour at different population and number of coefficient for Seed=1(a) and Seed=2(b).

Observations:

- The cost function is lower for the test cases that involve the higher number of coefficient and the higher population;
- In Fig. 28(b) it is shown (for the case P=40, K=400) that the cost function is still decreasing, so we propose to repeat the test cases increasing the maximum number of iteration to $I = 10^5$.

More information on the topics of this document can be found in the following list of references.

References

[1] M. Salucci, G. Oliveri, M. A. Hannan, and A. Massa, "System-by-design paradigm-based synthesis of complex systems: The case of spline-contoured 3D radomes," *IEEE Antennas and Propagation Magazine - Special Issue on 'Artificial Intelligence in Electromagnetics,'*, vol. 64, no. 1, pp. 72-83, Feb. 2022.

[2] G. Oliveri, P. Rocca, M. Salucci, and A. Massa, "Holographic smart EM skins for advanced beam power shaping in next generation wireless environments," *IEEE J. Multiscale Multiphysics Comput. Tech.*, vol. 6, pp. 171-182, Oct. 2021.

[3] G. Oliveri, A. Gelmini, A. Polo, N. Anselmi, and A. Massa, "System-by-design multi-scale synthesis of task-oriented reflectarrays," *IEEE Trans. Antennas Propag.*, vol. 68, no. 4, pp. 2867-2882, Apr. 2020.

[4] M. Salucci, L. Tenuti, G. Gottardi, A. Hannan, and A. Massa, "System-by-design method for efficient linear array miniaturisation through low-complexity isotropic lenses," *Electronic Letters*, vol. 55, no. 8, pp. 433-434, May 2019.

[5] M. Salucci, N. Anselmi, S. Goudos, and A. Massa, "Fast design of multiband fractal antennas through a system-by-design approach for NB-IoT applications," *EURASIP J. Wirel. Commun. Netw.*, vol. 2019, no. 1, pp. 68-83, Mar. 2019.

[6] M. Salucci, G. Oliveri, N. Anselmi, and A. Massa, "Material-by-design synthesis of conformal miniaturized linear phased arrays," *IEEE Access*, vol. 6, pp. 26367-26382, 2018.

[7] M. Salucci, G. Oliveri, N. Anselmi, G. Gottardi, and A. Massa, "Performance enhancement of linear active electronically-scanned arrays by means of MbD-synthesized metalenses," *Journal of Electromagnetic Waves and Applications*, vol. 32, no. 8, pp. 927-955, 2018.

[8] G. Oliveri, M. Salucci, N. Anselmi and A. Massa, "Multiscale System-by-Design synthesis of printed WAIMs for waveguide array enhancement," *IEEE J. Multiscale Multiphysics Computat. Techn.*, vol. 2, pp. 84-96, 2017.

[9] A. Massa and G. Oliveri, "Metamaterial-by-Design: Theory, methods, and applications to communications and sensing - Editorial," *EPJ Applied Metamaterials*, vol. 3, no. E1, pp. 1-3, 2016.

[10] G. Oliveri, F. Viani, N. Anselmi, and A. Massa, "Synthesis of multi-layer WAIM coatings for planar phased arrays within the system-by-design framework," *IEEE Trans. Antennas Propag.*, vol. 63, no. 6, pp. 2482-2496, June 2015.

[11] G. Oliveri, L. Tenuti, E. Bekele, M. Carlin, and A. Massa, "An SbD-QCTO approach to the synthesis of isotropic metamaterial lenses," *IEEE Antennas Wireless Propag. Lett.*, vol. 13, pp. 1783-1786, 2014.

[12] A. Massa, G. Oliveri, P. Rocca, and F. Viani, "System-by-Design: a new paradigm for handling design complexity," *8th European Conference on Antennas Propag. (EuCAP 2014), The Hague, The Netherlands*, pp. 1180-1183, Apr. 6-11, 2014.

[13] P. Rocca, M. Benedetti, M. Donelli, D. Franceschini, and A. Massa, "Evolutionary optimization as applied to inverse problems," *Inverse Problems - 25 th Year Special Issue of Inverse Problems, Invited Topical Review*, vol. 25, pp. 1-41, Dec. 2009.

[14] P. Rocca, G. Oliveri, and A. Massa, "Differential Evolution as applied to electromagnetics," *IEEE Antennas Propag. Mag.*, vol. 53, no. 1, pp. 38-49, Feb. 2011.

[15] M. Salucci, G. Gottardi, N. Anselmi, and G. Oliveri, "Planar thinned array design by hybrid analytical-stochastic optimization," *IET Microwaves, Antennas & Propagation*, vol. 11, no. 13, pp. 1841-1845, Oct. 2017

[16] G. Oliveri, M. Donelli, and A. Massa, "Genetically-designed arbitrary length almost difference sets," *Electronics Letters*, vol. 5, no. 23, pp. 1182-1183, Nov. 2009.

[17] P. Rocca, N. Anselmi, A. Polo, and A. Massa, "Pareto-optimal domino-tiling of orthogonal polygon phased arrays," *IEEE Trans. Antennas Propag.*, vol. 70, no. 5, pp. 3329-3342, May 2022.

[18] P. Rocca, N. Anselmi, A. Polo, and A. Massa, "An irregular two-sizes square tiling method for the design of isophoric phased arrays," *IEEE Trans. Antennas Propag.*, vol. 68, no. 6, pp. 4437-4449, Jun. 2020.

[19] P. Rocca, N. Anselmi, A. Polo, and A. Massa, "Modular design of hexagonal phased arrays through diamond tiles," *IEEE Trans. Antennas Propag.*, vol.68, no. 5, pp. 3598-3612, May 2020.

[20] N. Anselmi, L. Poli, P. Rocca, and A. Massa, "Design of simplified array layouts for preliminary experimental testing and validation of large AESAs," *IEEE Trans. Antennas Propag.*, vol. 66, no. 12, pp. 6906-6920, Dec. 2018.

[21] N. Anselmi, P. Rocca, M. Salucci, and A. Massa, "Contiguous phase-clustering in multibeam-on-receive scanning arrays," *IEEE Trans. Antennas Propag.*, vol. 66, no. 11, pp. 5879-5891, Nov. 2018.

[22] G. Oliveri, G. Gottardi, F. Robol, A. Polo, L. Poli, M. Salucci, M. Chuan, C. Massagrande, P. Vinetti, M. Mattivi, R. Lombardi, and A. Massa, "Co-design of unconventional array architectures and antenna elements for 5G base station," *IEEE Trans. Antennas Propag.*, vol. 65, no. 12, pp. 6752-6767, Dec. 2017.

[23] N. Anselmi, P. Rocca, M. Salucci, and A. Massa, "Irregular phased array tiling by means of analytic schemata-driven optimization," *IEEE Trans. Antennas Propag.*, vol. 65, no. 9, pp. 4495-4510, September 2017.

[24] N. Anselmi, P. Rocca, M. Salucci, and A. Massa, "Optimization of excitation tolerances for robust beamforming in linear arrays," *IET Microwaves, Antennas & Propagation*, vol. 10, no. 2, pp. 208-214, 2016.

[25] P. Rocca, R. J. Mailloux, and G. Toso, "GA-Based optimization of irregular sub-array layouts for wideband phased arrays desig," *IEEE Antennas and Wireless Propag. Lett.*, vol. 14, pp. 131-134, 2015.

[26] P. Rocca, M. Donelli, G. Oliveri, F. Viani, and A. Massa, "Reconfigurable sum-difference pattern by means of parasitic elements for forward-looking monopulse radar," *IET Radar, Sonar & Navigation*, vol 7, no. 7, pp. 747-754, 2013.

[27] P. Rocca, L. Manica, and A. Massa, "Ant colony based hybrid approach for optimal compromise sum-difference patterns synthesis," *Microwave Opt. Technol. Lett.*, vol. 52, no. 1, pp. 128-132, Jan. 2010.

[28] P. Rocca, L. Manica, and A. Massa, "An improved excitation matching method based on an ant colony optimization for suboptimal-free clustering in sum-difference compromise synthesis," *IEEE Trans. Antennas Propag.*, vol. 57, no. 8, pp. 2297-2306, Aug. 2009.

[29] P. Rocca, L. Manica, and A. Massa, "Hybrid approach for sub-arrayed monopulse antenna synthesis," *Electronics Letters*, vol. 44, no. 2, pp. 75-76, Jan. 2008.

[30] P. Rocca, L. Manica, F. Stringari, and A. Massa, "Ant colony optimization for tree-searching based synthesis of monopulse array antenna," *Electronics Letters*, vol. 44, no. 13, pp. 783-785, Jun. 19, 2008.

[31] M. Salucci, F. Robol, N. Anselmi, M. A. Hannan, P. Rocca, G. Oliveri, M. Donelli, and A. Massa, "S-Band spline-shaped aperture-stacked patch antenna for air traffic control applications," *IEEE Tran. Antennas Propag.*, vol. 66, no. 8, pp. 4292-4297, Aug. 2018.

[32] T. Moriyama, F. Viani, M. Salucci, F. Robol, and E. Giarola, "Planar multiband antenna for 3G/4G advanced wireless services," *IEICE Electronics Express*, vol. 11, no. 17, pp. 1-10, Sep. 2014.

[33] F. Viani, "Dual-band sierpinski pre-fractal antenna for 2.4GHz-WLAN and 800MHz-LTE wireless devices," *Progress In Electromagnetics Research C*, vol. 35, pp. 63-71, 2013.

[34] F. Viani, M. Salucci, F. Robol, and A. Massa, "Multiband fractal Zigbee/WLAN antenna for ubiquitous wireless environments," *Journal of Electromagnetic Waves and Applications*, vol. 26, no. 11-12, pp. 1554-1562. 2012.

[35] F. Viani, M. Salucci, F. Robol, G. Oliveri, and A. Massa, "Design of a UHF RFID/GPS fractal antenna for logistics management," *Journal of Electromagnetic Waves and Applications*, vol. 26, pp. 480-492, 2012.

[36] M. Salucci, L. Poli, A. F. Morabito, and P. Rocca, "Adaptive nulling through subarray switching in planar antenna arrays," *Journal of Electromagnetic Waves and Applications*, vol. 30, no. 3, pp. 404-414, February 2016

[37] T. Moriyama, L. Poli, and P. Rocca, "Adaptive nulling in thinned planar arrays through genetic algorithms," *IEICE Electronics Express*, vol. 11, no. 21, pp. 1-9, Sep. 2014.

[38] L. Poli, P. Rocca, M. Salucci, and A. Massa, "Reconfigurable thinning for the adaptive control of linear arrays," *IEEE Trans. Antennas Propag.*, vol. 61, no. 10, pp. 5068-5077, Oct. 2013.

[39] P. Rocca, L. Poli, G. Oliveri, and A. Massa, "Adaptive nulling in time-varying scenarios through time-modulated linear arrays," *IEEE Antennas Wireless Propag. Lett.*, vol. 11, pp. 101-104, 2012.

[40] F. Viani, F. Robol, M. Salucci, and R. Azaro, "Automatic EMI filter design through particle swarm optimization," *IEEE Trans. Electromagnet. Compat.*, vol. 59, no. 4, pp. 1079-1094, Aug. 2017.

[41] G. Oliveri, M. Salucci, and A. Massa, "Towards reflectarray digital twins - An EM-driven machine learning perspective," *IEEE Transactions on Antennas and Propagation - Special Issue on 'Machine Learning in Antenna Design, Modeling, and Measurements,'* vol. 70, no. 7, pp. 5078-5093, July 2022.

[42] M. Salucci, L. Tenuti, G. Oliveri, and A. Massa, "Efficient prediction of the EM response of reflectarray antenna elements by an advanced statistical learning method," *IEEE Trans. Antennas Propag.*, vol. 66, no. 8, pp. 3995-4007, Aug. 2018.